# Rock-physics-assisted interpretation of elastic property of the geological environments in the Buzios field, Brazilian pre-salt.

Leonardo Teixeira, Maria Taryn Relvas Campos, Julia Guerrero, Victor Mund, Mônica Muzzete, Fátima Brazil, Carlos Eduardo Abreu, Petrobras.



This paper was prepared for presentation during the 18th International Congress of the Brazilian Geophysical Society held in Rio de Janeiro, Brazil, 16-19 October 2023.



Carbonate platform interpretation advances rely on seismic amplitude to identify geomorphology and infer depositional systems. Nonetheless, the same stratigraphic architecture can be susceptible to post-depositional diageneses that drastically alter reservoir quality, potentially unnoticed by seismic facies. Furthermore, the calibration of rock-physics models for presalt carbonates reveals that acoustic impedance is mainly affected by porosity changes, whereas Vp/Vs is affected by mineralogy variations, shedding light on new possibilities of seismic interpretations. This work describes four types of facies: silica-rich, calcite-rich, dolomite-rich, and clay-bearing facies to study the elastic property geomorphology of geological environments. We highlight the advantages of employing seismic-derived acoustic impedance and Vp/Vs in interpreting geological settings, poorly documented in the literature for presalt reservoirs. This methodology describes a practical seismic-mappable procedure for determining the sedimentological control and geographical distribution of diagenetic processes in the Buzios field. We show that using rock physics to interpret seismic-derived acoustic impedance and Vp/Vs is a reliable way to forecast mineralogical alteration and porosity quality, whose predictability is confirmed by blind wells. We advocate that this analysis is expandable to other presalt reservoirs.

## Introduction

The Búzios Field, located in the oil-prolific Santos Basin, is a world-class field responsible for the second-largest oil production in Brazil, reaching 490 Mbbl/d on March 2023, and accounting for 21% of total national production (ANP, 2023). The ring fence has a total area of 852.2 $km^2$ and contains an estimated 24.24 billion barrels of proven plus probable and possible reserves (ANP, 2021).

Interpretation of seismic data is primarily performed on seismic amplitude. Since the seminal paper of AAPG Memoir (Vail et al., 1977; Mitchum et al., 1977), geophysicists have been looking for geological patterns that resemble depositional environments to associate them with depositional sequences and, thus, the facies-filling sediments. The geomorphology of seismic signals, known as seismic facies, is a toolkit for interpreting carbonate platforms, reasoning about depositional and diagenetic processes (Hendry et al., 2021; Oliveira et at, 2021).

Seismic amplitude patterns also underpin the interpretation of carbonate pre-salt reservoirs, alluding to the depositional environments and facies associations (Macedo et al., 2021; Adriano et al., 2022). Furthermore, seismic attributes based on amplitude transformation assist seismic interpretation, clarifying and simplifying the recognition of geomorphological patterns in these reservoirs (Buckley et al., 2015; Ferreira et al., 2021). Notwithstanding the advance in amplitude to the identification of geological settings, ultrasonic laboratory and well-log analysis evidence that potential understanding of depositional and diagenetic processes lurks within the elastic properties.

Rock-physics analysis evidences that porosity, mineralogical content, and poro shape primarily influence the response of elastic properties in pre-salt reservoirs (Vasquez et al., 2019; Silva et al., 2020; Dias et al., 2021). Therefore, some authors propose elastic-property-sensitive facies classification based on porosity range and clay content (Teixeira et al., 2017), flow unit (Penna and Lupinacci, 2020), and mineralogy (Mello and Lupinacci, 2022), essentially to discretize those facies to extend them to seismic classification.

We follow the previous understanding to categorize the presalt facies based on clay content and mineralogy to interpret the elastic response in seismic volumes in the Itapema and Barra Velha Formations. We use ultrasonic laboratory measurements to construct the rock-physics template in order to translate the effect of elastic property variations, noticed in seismic data, into reservoir property. We calibrate rock-physics models to demonstrate that acoustic impedance responds to porosity changes while Vp/Vs is mineralogy-related changes.

This paper produces four descriptions of facies: silica-rich, calcite-rich, dolomite-rich, and clay-bearing facies. Nevertheless, instead of using these facies for supervised classification, this study focuses on geomorphology patterns of elastic responses. Seismic amplitude recognizes geological environments. However, similar stratigraphic architecture can be susceptible to post-depositional diageneses that significantly change reservoir quality which can be unclear in seismic amplitude. Here, we prove that the rock-physic-assisted interpretation of seismic-derived acoustic impedance and Vp/Vs is a robust complement to predict how diagenesis processes act on the reservoir porosity. Also, this methodology provides a seismic-mappable toolkit to infer the sedimentological control and the spatial distribution of the diagenetic process in the Búzios field, which is still poorly understood. Blind wells testify to the predictions on silicification and porosity quality.

**Geological Settings**

The Santos Basin is the largest salt basin offshore Brazil, whose history starts with the break-up of Gondwana in the Early Cretaceous, which progress led to the opening of the Atlantic Ocean (Moreira et al., 2007; Kukla et al., 2018). The Santos Basin covers an area of about 350,000 km$^2$ and is bounded by the Florianopolis High to the south and the Cabo Frio High to the north. In this context, the Buzios field, positioned in the north-central area of the basin, is about 180 km off the Brazilian continental margin.

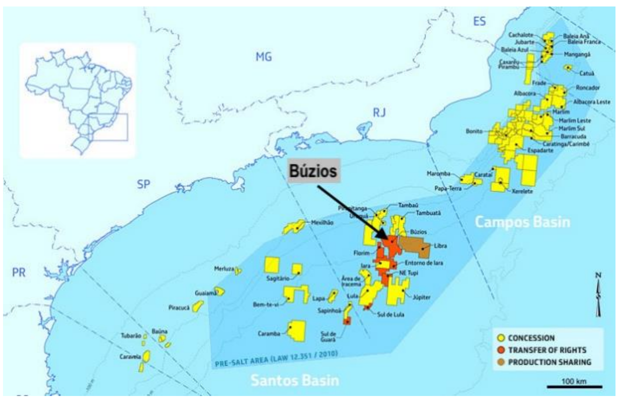

Figure 1 – Location of the Búzios Field in the Santo Basin.

The Buzios Field comprises carbonate rocks from The Barra Velha Formation (BVE) and the Itapema Formation (ITP). The Itapema Formation is mainly composed by rudstones to grainstones formed by bivalve shells, informally known as coquinas. These shells were mechanically transported, fragmented, and deposited in the structural highs during the Barremian to Aptian rift (Oliveira et al., 2021). In this formation, the lake-level fluctuations and storm-related events control the deposition of these rocks (Oliveira et al., 2021; Lupinnaci et al., 2023). Some important seismofacies have been identified in the Búzios field, such as Platform Edge Clinoforms and Deep Lake Siltstones (Campos et al., 2022). Two significant unconformities involve the Itapema Formation: one the at the base, related to Piçarras Formation, and one at the top, which marks the beginning of the deposition of the Barra Velha Formation (Moreira et al., 2007).

The Barra Velha Formation is composed of shrubs, spherulites, and Mg-clay-rich muds deposited in a relatively shallow, hyperalkaline, lacustrine environment during the Aptian (Wright and Rodriguez, 2018; Gomes et al., 2020), divided into two intervals: the sag phase (BVE100, BVE200), the upper interval, and the rift phase (BVE300), the lower interval. The interpretation of seismic data identifies that these facies are sedimented in major geological domains such as mounds, debris flows, reworked coastal ridges, and bottom-lake deposits (Ferreira et al., 2021; Campos et al., 2022).

**Dataset**

The dataset consists of Ocean Bottom Nodes (OBN) data whose nodes were deployed in every 500 m in a staggered configuration with shots 50m apart in a flip-flop configuration (Martinez et al., 2020). The final seismic image includes the application of full-waveform inversion (FWI) to derive the velocity model for the least-square reserve-time migration (LSRTM). The angle gathers were stacked in four volumes: 03-13 (near), 11-21 (mid), 19-29 (far), and 27-37 (ultrafar). The seismic signal polarity follows the SEG (Society of Exploration Geophysical) convention, which considers the positive amplitude as an increase of acoustic impedance in the interface of two layers and the negative amplitude as a decrease.

The dataset comprises logs from over 60 wells recording properties of the Itapema and Barra Velha Formations. The set of logs contains neutron and nuclear resonance magnetic porosities, density, sonic, gamma ray, and litogeochemistry. Additionally, the dataset includes laboratory porosity measurements, ultrasonic velocities, and x-ray diffractions.

**Method**

The method composes the integrated interpretation of the rock-physics analysis and the seismic-derived elastic properties in a workflow known as quantitative seismic interpretation. Prior to the evaluation of the rock-physics analysis, we interpreted the predominant mineralogy facies classification to understand how dolomitization and silicification act on the elastic response.

**Facies classification**

This paper proposes the mineralogy-based facies classification in four rock types: calcite-rich facies, clay-bearing facies, dolomite-rich facies, and silica-rich facies. The nuclear magnetic resonance logs (NMR) support the identification of the clay-bearing facies in carbonate rocks because, in these formations, the free-fluid porosity detaches significantly from the total porosity. The calcite-, dolomite-, and silica-rich facies follow the interpretation of lithogeochemistry logs which determine the predominant mineralogy. First, the clay-bearing facies is classified. Essentially, these are non-reservoir rocks. In reservoir rocks, which exclude the clay-bearing facies, the lithogeochemistry logs indicate the prevalent mineral and, consequently, the calcilte-, dolomite-, and silica-rich facies.

**Rock-physics Analysis**

This analysis studies how the changes in reservoir properties affect the elastic properties (Dvorkin et al, 2014). To this end, we analyze information from porosity and ultrasonic laboratory measurements and well logs and confront them with theoretical and empirical rock-physics templates. The ray-X diffraction and lithogeochemistry logs support the quantification of the mineralogical content, while thin sections allow for the qualitative inspection of the aspect ratio of the porous geometry. This information is critical for rock-physics modeling and the interpretation of seismic-derived elastic properties.

**Seismic inversion to elastic properties**

The inversion process starts with an initial model to fill the low-frequency bandwidth absent in seismic data generated by well-log interpolation following the stratigraphic grid of the interpreted pre-salt horizons (base of salt, BVE300, Jiquia mark, base of reservoir, basement). The method assumes that the seismic reflectivity (parameter model) is sparse and spiky using the L-1 norm, and the residue (difference between modeled and real data) is normally distributed using the L-2 norm (Wang et al. 2017). The algorithm modifies the initial low-frequency model to minimize the difference between the synthetic and observed seismic data until it reaches a satisfactory error (Latimer 2011).

Since the procedure aims at estimating the elastic properties, the low-frequency models contain the seismic volumes of acoustic impedance, compressional-to-shear velocity ratio, and density. The estimation of the wavelet is angle-dependent; therefore, we assess four wavelets, one for each angle stack. The quality control follows conventional inversion standards, which involve comparing synthetic and observed data, well-log elastic properties, and pseudolog extracted from seismic volumes and analysis signal-to-noise ratio (SNR) (Kemper, 2010).

**Results**

Predominant mineralogical facies interpretation based on well logs is the starting point of our methodology. Figure 2 exemplifies the predominant mineralogical facies interpretation in well 9-RJS-709. The process starts off with the interpretation of the clay-bearing facies based on the detachment of the free-fluid porosity and total porosity in the NMR log. The method advanced with the identification of the predominant mineralogical porosity based on the lithogeochemistry log. This results in the interpretation of silica-rich (yellow), dolomite-rich (purple) and calcite-rich (blue) facies. The clay-bearing facies at the top of the Itapema Formation represents the detritic deposition of the Jiquia Shales, determined by high Gamma Ray, and marks the onset of this formation.

We proceed with the rock-physics analysis. Figure 3 displays the crossplot of the porosity and dry bulk moduli, measured by ultrasonic laboratory device, in calcite-dominated samples. The plot also exhibits the modeling of the Differential Effective Medium (DEM) to fully understand the behavior of the influence of porous geometry in elastic response (Mukerji et al., 1995; Saxena et al., 2018). The rock-physics template suggests that the effective aspect ratio lies between 0.1 and 0.2.

This analysis teaches us how to broaden the Differential Effective Medium (DEM) by altering the prevalent mineralogical compositions. For example, in the scatter plot of Vp/Vs *versus* acoustic impedance color-coded by the dominant mineralogy, the rock-physics template includes silica-rich (yellow) and dolomite-rich (dark blue) content, with an effective aspect ratio of 0.16 (Figure 4).

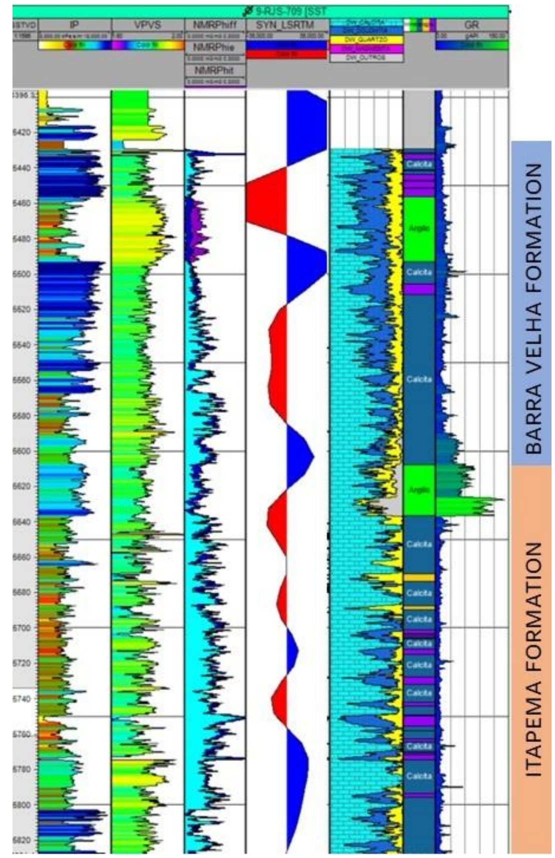


Figure 2 – Well 9-RJS-709. From left to right. acoustic impedance, compressional-to-shear velocity ratio (Vp/Vs), NMR porosity, synthetic seismic, the accumulative lithogeochemistry log, the interpretation of predominant mineralogical facies, and gamma ray log. Key color: silica-rich (yellow), dolomite-rich (purple), calcite-rich (blue), clay-bearing (green) facies.

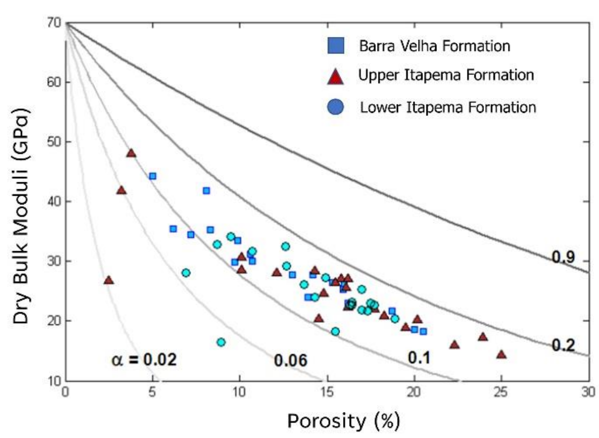


Figure 3 – Rock-physics template modeling the Differential Effective Medium (DEM) in calcite-dominated samples. The lines represent the aspect ratios (modified from Morschbacher, 2016).

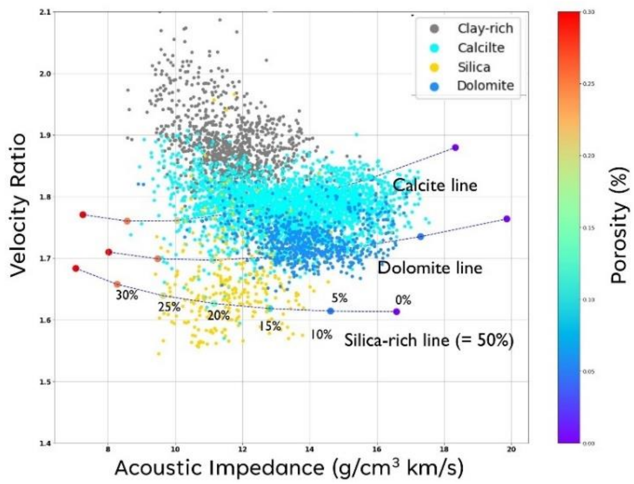


Figure 4 – Rock-physics template for the Buzios field. The lines represent the modeling of the Differential Effective Medium (DEM) in oil-bearing log samples, varying the mineralogical content and porosity.

Figures 5 and 6 show the volumes of acoustic impedance and Vp/Vs produced by the sparse-spike inversion. Along with the seismic section, Well A depicts the well path color-coded by the respective elastic property. The comparison between the seismic volume and well-log-based property demonstrates a high correlation of the seismic inversion. As expected, the acoustic impedance exhibits superior quality, higher correlation, and continuity than the Vp/Vs volume; yet, the Vp/Vs provides steady and interpretable results.

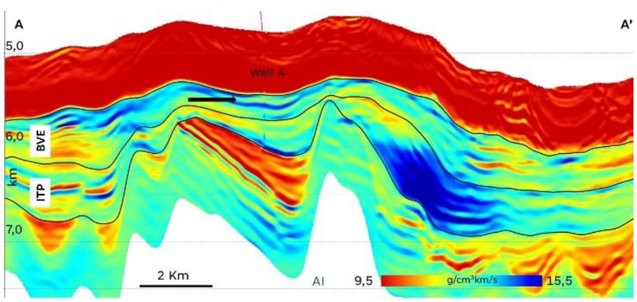


Figure 5 – Seismic-derived acoustic impedance and the trajectory of well A, color-coded by the respective property. The comparison between the seismic volume and well-log-based property demonstrated the high quality of the seismic inversion.

## Interpretations and discussions

This paper embraces the concept of classifying the facies for the elastic property interpretation based on the prevalent mineralogy. This assumption is relevant for the pre-salt since the deposition facies of these carbonates are indistinguishable by the elastic properties. Other classifications have been proposed on the basis of porosity cut-offs (Teixeira et al., 2017; Oliveiwagra et al., 2018; Penna et al., 2019) or the mix of mineralogy (Mello and Lupinacci, 2022), chiefly to extend the classification to the seismic volume. Since this work focuses on interpreting elastic response partners, the predominantly mineralogical assembly is suitable.

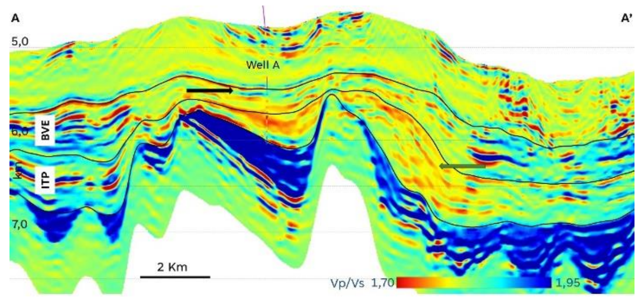


Figure 6 – Seismic-derived Vp/Vs and the trajectory of well A, color-coded by the respective property. The comparison between the seismic volume and well-log-based property demonstrated the good quality of the seismic inversion.

The analysis of the ultrasonic laboratory measurement depicts scattered points between the aspect ratio of 0.1 and 0.2 (Figure 3), indicating that the effective aspect ratio lies between these bounds. The rock-physics templates, tailored by oil-bearing samples of well logs, suggest that 0.16 explains the elastic property behavior of these reservoirs and, therefore, is a reasonable choice. This value is close to the suggestion of 0.18 for other presalt field (Silva et al, 2020). Nonetheless, one must bear in mind that the effective aspect ratio is a simplification. The matrix of the pre-salt reservoir possibly behaves as a distribution of compliant and stiff aspect ratios (Dias et al., 2020)

Yet a simplification, the rock-physics templates provide solid foundations for interpreting the elastic patterns. It reveals that the acoustic impedance is sensitive to the porosity changes, whereas Vp/Vs is essentially a response of the predominant mineralogy. As the reservoir is calcite-dominated carbonate, the silicification results in a relative reduction in Vp/Vs, to around 1.65. The decrease in Vp/Vs by dolomitization of calcite-rich facies is small, thus, the detection in seismic-derived elastic property is very noise-sensitive and possibly implausible. If the dolomitization obliterates the porous medium, acoustic impedance increases; otherwise, it decreases. In addition, the inclusion of clay content in the matrix increases Vp/Vs and reduces acoustic impedance.

Figure 7 shows the mean acoustic impedance for the upper interval of the Barra Velha Formation. It exemplifies how powerful rock-physics-assisted interpretation can be in mapping reservoir diagenesis. In this figure, 2-ANP-1 has a very high impedance (> 15.5), manifesting, according to the rock-physics template, very low porosity (a detailed analysis of this well can be found in Mallet and Lupinacci, 2022). Well C and Well D express similar values on the map. The low porosities in these three wells are related to the dolomitization that decreased the porosity. The map reveals the extension of the diagenetic process. Well 708 comprises calcite-rich high-porosity facies, explaining the low acoustic impedance. Downwards to Well 709, the map indicates that acoustic impedance rises, a reduction in porosity. In Well 709, a restricted structural low, low acoustic impedance is related to the increase in clay content. This transitional environment, low to high to low acoustic impedance, reflects in the seismic section as a geological aspect known as feature “X”. The occurrence was first interpreted in the Tupi field (Cruz et al., 2021).

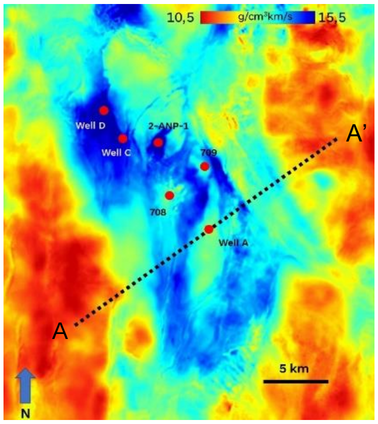


Figure 7 – Mean acoustic impedance of the upper Barra Velha Formation. The dashed line represents the seismic section in Figures 5 and 6.

The rock-physics templates show that the high-porosity facies (Well 708) and clay-bearing carbonates (Well A) present low acoustic impedance; however they are in two different geological reliefs. Well A resides in a structural low limited by two highs, indicating a restricted system dominated by low-energy deposits (black arrow in Figure 5). As a result, the interpretation of concave-shaped low acoustic impedance in these relative lows is more prone to clay-bearing facies than to high-porosity carbonates. In contrast, high Vp/Vs indicates clay-bearing facies, providing additional information to reduce the uncertainty in the identification of these low-quality reservoir rocks (black arrow in Figure 6).

The silica-rich facies in the rock-physics template have low acoustic impedance and low Vp/Vs. It turns out that silicification increases the porosity in wells used to compose the template. Nevertheless, the model predicts that if the silicification reduces porosity, acoustic impedance increases, and Vp/Vs remains low.

To inspect the rock-physics predictability in unnoticed facies, Figures 08 and 09 illustrated a depth slice of acoustic impedance and Vp/Vs, respectively, crossing the lower interval of the Itapema Formation. Well E and Well F are blind wells in clinoform-shaped amplitudes that drilled moderate-to-high energy coquinas. However, both exhibit very different elastic patterns. Well E presents a lateral cyclicity of low Vp/Vs while acoustic impedance has constantly high values. That leads to the plausible prediction that this interval is dominated by cycles of silicification that reduced the porosity. Meanwhile, Well F has moderate-to-high cycles of acoustic impedance and moderate constant Vp/Vs, suggesting cycles of low-to-moderate porosity and negligible silicification. Both wells confirm the seismic prediction.

The analysis of elastic property patterns complements the conventional amplitude interpretation of the pre-salt geological environments. For example, the green arrow in Figure 06 shows how the Vp/Vs alternates vertically and laterally, following the Itapema Formation's clinoforms. This information, together with well data, suggests that the silicification is stratigraphically induced and seismically mappable.

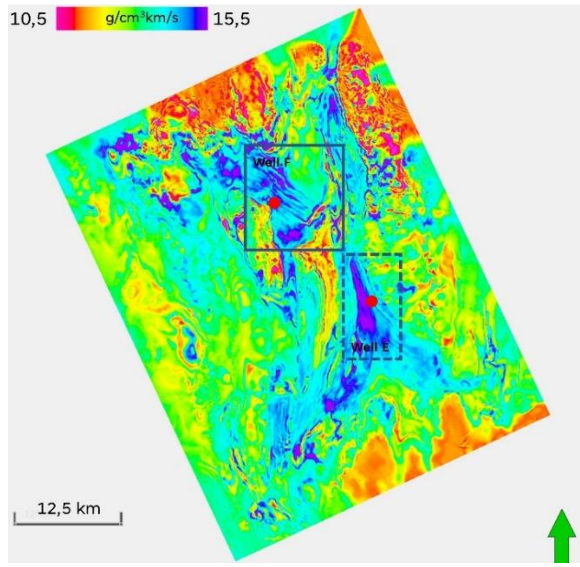


Figure 08 – Depth slice of acoustic impedance in the lower interval of the Itapema Formation. The dashes box contains constantly high acoustic impedance whereas the solid box contains laterally variable cycles of moderate-to-high acoustic impedance.

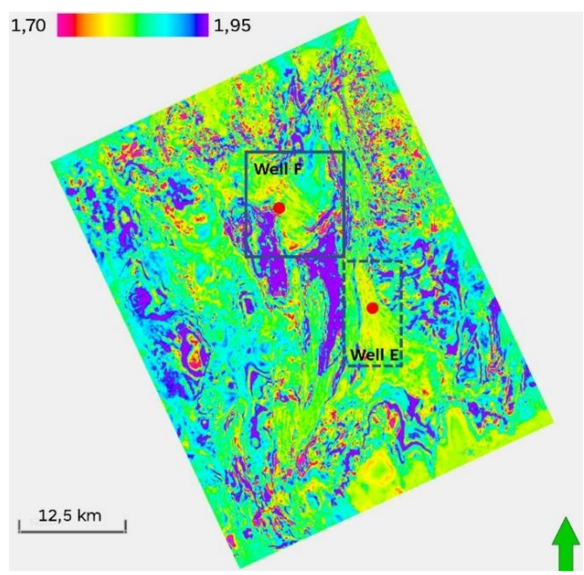


Figure 09 – Depth slice of Vp/Vs in the lower interval of the Itapema Formation. The dashes box contains laterally variable cycles of low-to-moderate Vp/Vs whereas the solid box contains laterally variable cycles of near-constant moderate Vp/Vs.

**Conclusions**

- By applying the differential effective medium, the rock-physics template suggests that the aspect ratio of pre-salt rocks lies between 0.1 and 0.2. Therefore, we find 0.16 a suitable value for the Buzios field.
- In a pre-salt reservoir, variation of acoustic impedance is related to variation of porosity, whereas Vp/Vs is related to changes in predominant mineralogical content.
- Steady seismic-derived Vp/Vs reduces the uncertainty in estimating clay-bearing facies.
- The reduction in Vp/Vs by dolomitization of calcite-rich facies is smaller than the silicification-induced reduction; thus, the detection in elastic property volumes of dolomite-rich facies is very noise-sensitive and possibly implausible.
- Vertical and lateral alternations of Vp/Vs in the Itapema Formation's clinoforms suggest that the silicification is stratigraphically induced and seismically mappable.
- Seismic amplitude is robust in identifying geological features to infer the structure-filling sediments and facies association. Herein, we prove that the seismic-derived elastic property is an additional, indispensable data to map the extension of the reservoir quality and diagenetic process.

**Acknowledgments**

The authors thank Petrobras, CNOON, and CNODC for allowing the public presentation of this work. Also, the authors recognize externally unpublished articles presented at in-house symposiums that significatively contributed to the development of this study. In this context, we thank Ana Moliterno, Lucia Dillon, and Guenther Neto for pioneering interpretations in the Buzios field.

**References**

ADRIANO, M.; FIGUEREDO, J.; COELHO, P.; BORGUI, L. 2022. Tectonic and stratigraphic evolution of the Santos Basin rift phase: New insights from seismic interpretation on Tupi oil field area. Journal of South American Earth Science, 116. Doi:10.1016/j.jsames.2022.103842

ANP. 2016. Plano de desenvolvimento econômico de Búzios. ANP.

ANP. 2023. Boletim da produção de petroléo e gás natural. ANP.

BUCKLEY, J. P.; BOSENCE, D.; ELDERS, C. 2015. Tectonic setting and stratigraphic architecture of an Early Cretaceous lacustrine carbonate platform, Sugar Loaf High, Santos Basin, Brazil. Geological Society, London, Special Publications, 418(1), 175–191. doi:10.1144/sp418.13

CAMPOS, T; SILVA, E.; GUERRERO, J. 2022. Seismofacies interpretation and implications for the production geological model: examples from the Buzios Field. Fourth EAGE/HGS Conference on Latin America.

CHINELATTO, G.; BALILA, A.; BASSO, M.; SOUZA, J.; VIDAL, A. 2020. A taphofacies interpretation of shell concentrations and their relationship with petrophysics: a case study of Barremian-Aptian coquinas in the Itapema Formations, Santos Basin, Brazil. Marine and Petroleum Geology, 116. Doi: 10.1016/j.marpetgeo.2020.104317

CRUZ, N., CRUZ, J.; MUZZETE, M.; URASAKI, E.; TEIXEIRA, L.; GROCHAU, M., 2021, First 4D seismic results for Tupi Field, Santos Basin: International Congress of the Brazilian Geophysical Society.

DIAS, J.; LOPEZ, J.; VELLOSO, R,; PEROSI, F. 2022. A workflow for multimineralogic carbonate rock physics modelling in a Bayesian framework: Brazilian pre-salt reservoir case study. Geophysical Prospecting, 69. doi:10.1111/1365-2478.13060

DVORKIN, J., GUTIERREZ, M.; GRANA, D. 2014. Seismic reflections of rock properties: Cambridge.

FERREIRA, F.; DIAS, R.; LUPINACCI, W. 2021. Seismic pattern classification integrated with permeability-porosity evaluation for reservoir characterization of presalt carbonates in the Buzios Field, Brazil. Journal of Petroleum Science and Engineering, 201. Doi: https://doi.org/10.1016/j.petrol.2021.108441

FERREIRA, D.; DUTRA, H.; CASTRO, T.; LUPINACCI, W. 2021. Geological process modeling and geoestatistics facies reconstruction of presalt carbonates. Marine and Petroleum Geology, 124. Doi: https://doi.org/10.1016/j.marpetgeo.2020.104828

HENDRY, J.; BURGESS, P.; HUNT, D.; ZAMPETTI, V. 2021. Seismic Characterization of carbonate platforms and Reservoirs. Special Publication, Geological Society of London. Doi: https://doi.org/10.1144/SP509

GOMES, J., BUNEVICH, R.; TEDESCHI, L.; TUCKER, M.; WHITAKER, F. 2020. Facies classification and patterns of lacustrine carbonate deposition of the Barra Velha Formation, Santo Basin, Brazilian pre-salt: Marine and Petroleum Geology, 113, 104176, doi:10.1016/j.marpetgeo.2019.104176.

KEMPER, M. 2010. Rock physics driven inversion: the importance of workflow. First Break, 28.

KUKLA, P.A., STROZYK, F., MOHRIAK, W.U. 2018. South Atlantic salt basins 1 witnesses of complex passive margin evolution. Gondwana Research, 53, 41–57. https://doi.org/ 10.1016/j.gr.2017.03.012.

LATIMER, R. 2011. Inversion and interpretation of impedance data. In: Interpretation of Three-Dimensional

Seismic Data.: Society of Exploration Geophysicists and American Association of Petroleum Geologists.

LUPINACCI, W.; FATAH, T.; CARMO, M.; FREIRE, A.; GAMBOA, L., 2023. Controls of fracutring in porosity in pre-salt carbonates. Energy Geoscience, 4. 2023. Doi: https://doi.org/10.1016/j.engeos.2022.100146

MACEDO, P.; BARRETO, D.; ABRANTES JR, F,; NEVES, I.; LUPINACCI, W,. 2021. Application of seismic architecture interpretation in pre-salt carbonate reservoirs of the Buzios field, Santos Basin, Offshore Brazil. Brazilian Journal of Geophysics, 39. Doi: http://dx.doi.org/10.22564/rbgf.v39i3.2110

MALLET, T.; LUPINACCI, W.; 2022. Comparison between conventional and NMR approaches for formation evaluation of presalt interval in the Buzios Field, Santos Basin, Brazil. Journal of Petroleum Science and Engineering, 208. doi:10.1016/j.petrol.2021.109679

MARTINEZ, A;, KHALIL, A.; OLIVEIRA, W.; NAOMITSU, E.; MOLITERNO, A. 2020. The potential of sparse nodes for exploration in Santos Basin. SEG Technical Program Expanded Abstracts doi: 10.1190/segam2020-3427880.1

MELLO, V. L.; LUPINACCI, W. 2022, Mineralogy based classification of carbonate rocks using elastic parameters: A case study from Buzios field: Journal of Petroleum Science and Engineering, 209, 109962, doi:10.1016/j.petrol.2021.109962.

MITCHUM, R. M., VAIL, P.; SANGREE, J. 1977, Seismic stratigraphy and global changes of sea level, part 6: Stratigraphic interpretation of seismic reflection patterns in depositional sequences: In Seismic Stratigraphy - Applications to Hydrocarbon Exploration.

MOREIRA, J.; MADEIRA, C; GIL, J.; PINHEIRO, M. 2007. Bacia de Santos. Boletim de Geociência d Petrobras.

MORSCHBACHER, M. 2016. Análise petrossísmica de plugues de testemunhos do campo de Búzios. CENPES.

MUKERJI, T.; BERRYMAN, J.; MAVKO, G; BERGE, P. 1995. Differential effective medium modeling of rock elastic moduli with critical porosity constraints. Geophysical Research Letters. doi: 10.1029/95GL00164

OLIVEIRA, L.; PIMENTEL, F.; PEIRO, M,; AMARAL, P.; CHRISTOVAN, J. 2018. A seismic reservoir characterization and porosity estimation workflow to support geological model update: pre-salt reservoir case study, Brazil, First Break, 36

OLIVEIRA, L.; RANCAN, C.; SARTORATO, A.; FARIAS, F.; PEREIRA, E. 2021. Drowing unconformities on presalt carbonate platforms – examples from the Itapema Formation (Lowe Cretaceous), Santos Basin, offshore Brazil. Palaeogeography, Paleoclimatology, Palaecology, 577. doi: http://dx.doi.org/10.1016/j.palaeo.2021.110570

PENNA, R., ARAÚJO, S., GEISSLINGER, A., SANSONOWSKI, R., OLIVEIRA, L., ROSSETO, J., MATOS, M. 2019. Carbonate and igneous rock characterization through reprocessing, FWI imaging, and elastic inversion of a legacy seismic data set in Brazilian presalt province. The Leading Edge, 38. doi:10.1190/tle38010011.1

PENNA, R., LUPINACCI, W. 2020. Decameter-Scale Flow-Unit Classification in Brazilian Presalt Carbonates. SPE Reservoir Evaluation & Engineering. doi:10.2118/201235-pa

SAXENA, V.; KRIEF, M.; ADAM, L. 2018. Handbook of borehole acoustic and rock physics for reservoir characterization. Elsevier.

SILVA, E.; DAVOLIO, A.; SANTOS, M; SCHIOZER, J. 2020. 4D petroelastic modeling based on a presalt well. Interpretation, 8, doi: 10.1190/INT-2019-0099.1

TEIXEIRA, L.; CRUZ, N.; SILVANY, P.; FONSECA, J.. 2017. Quantitative seismic interpretation integrated with well-test analysis in turbidite and presalt reservoirs: The Leading Edge, 36, no. 11, 931–937, doi:10.1190/tle36110931.1.

VAIL, P.; MITCHUM, R.; THOMPSON, S. 1977. Seismic stratigraphy and global changes of sea level, part 4: Global cycles of relative changes of sea level: In Seismic Stratigraphy - Applications to Hydrocarbon Exploration.

VASQUEZ, G. F.; . MORSCHBACHER, M.; DOS ANJOS, C,; SILVA, Y.; MADRUCCI, V.; JUSTEN, J. 2019. Petroacoustics and composition of presalt rocks from Santos Basin: The Leading Edge, 38. doi: 10.1190/tle38050342.1.

WANG, Y. 2017. Seismic inversion: theory and application. Wiley-Blackwell.

WRIGHT, V.P.; RODRIGUEZ, K. 2018. Reinterpreting the South Atlantic Pre Salt ‘Microbialite’ reservoirs: petrographic, isotopic and seismic evidence for ashallow evaporitic lake depositional model. First Break , 36 , 71–77, https://doi.org/10.3997/1365-2397.n0094